Resource

Immunity

GM-CSF Mouse Bone Marrow Cultures Comprise a Heterogeneous Population of CD11c^{+}MHCII^{+} Macrophages and Dendritic Cells

Highlights

- Mouse bone marrow cultured in GM-CSF generates dendritic cells (DCs) and macrophages
- Macrophages and DCs both express CD11c and MHC class II
- DCs arise from DC-committed progenitors and macrophages derive from monocytes
- DCs and macrophages can both undergo maturation but remain separable entities

Authors

Julie Helft, Jan Böttcher, Probir Chakravarty, ..., Barbara U. Schraml, Delphine Goubau, Caetano Reis e Sousa

Correspondence

caetano@crick.ac.uk

In Brief

Culture of bone marrow cells with cytokine GM-CSF is a widely used protocol to generate mouse dendritic cells (DCs). Reis e Sousa and colleagues show that monocyte-derived macrophages resembling immature DCs also develop in such cultures, which should be taken into account when using GM-CSF cultures to study DC biology.

Accession Numbers

GSE62361
GSE62746

Helft et al., 2015, Immunity *42*, 1197–1211
June 16, 2015
http://dx.doi.org/10.1016/j.immuni.2015.05.018

CellPress

Immunity
Resource

GM-CSF Mouse Bone Marrow Cultures Comprise a Heterogeneous Population of CD11c$^+$MHCII$^+$ Macrophages and Dendritic Cells

Julie Helft,[1] Jan Böttcher,[1] Probir Chakravarty,[2] Santiago Zelenay,[1] Jatta Huotari,[1] Barbara U. Schraml,[1,3] Delphine Goubau,[1] and Caetano Reis e Sousa[1,*]
[1]Immunobiology Laboratory
[2]Bioinformatics Laboratory
The Francis Crick Institute, Lincoln's Inn Fields Laboratory, 44 Lincoln's Inn Fields, London WC2A 3LY, UK
[3]Present address: Institute for Medical Microbiology, Immunology and Hygiene, Technische Universität München (TUM), Munich 81675, Germany
*Correspondence: caetano@crick.ac.uk
http://dx.doi.org/10.1016/j.immuni.2015.05.018

SUMMARY

Dendritic cells (DCs) are key players in the immune system. Much of their biology has been elucidated via culture systems in which hematopoietic precursors differentiate into DCs under the aegis of cytokines. A widely used protocol involves the culture of murine bone marrow (BM) cells with granulocyte-macrophage colony-stimulating factor (GM-CSF) to generate BM-derived DCs (BMDCs). BMDCs express CD11c and MHC class II (MHCII) molecules and share with DCs isolated from tissues the ability to present exogenous antigens to T cells and to respond to microbial stimuli by undergoing maturation. We demonstrate that CD11c$^+$MHCII$^+$ BMDCs are in fact a heterogeneous group of cells that comprises conventional DCs and monocyte-derived macrophages. DCs and macrophages in GM-CSF cultures both undergo maturation upon stimulation with lipopolysaccharide but respond differentially to the stimulus and remain separable entities. These results have important implications for the interpretation of a vast array of data obtained with DC culture systems.

INTRODUCTION

Dendritic cells (DCs) are sentinel leucocytes that reside in tissues and respond to pathogen entry by undergoing "maturation" and becoming competent to prime T cell responses (Banchereau and Steinman, 1998; Merad et al., 2013). DCs have traditionally been defined by phenotypic as well as functional characteristics. The former includes lack of expression of lineage-restricted markers and expression of the integrin CD11c and MHC class II (MHCII) molecules. Functional attributes include high motility and the ability to efficiently capture, process, and present antigens to T lymphocytes. This definition has become blurred of late by analyses that have underscored a marked degree of overlap between DCs and macrophages, including the ability of the latter to sometimes express MHCII and/or CD11c (Merad et al., 2013). It has prompted a move to distinguish members of the mononuclear phagocyte family on the basis of a different criterion, that of ontogeny (Guilliams et al., 2014). This notion comes from recent work demonstrating that the differentiation of DCs is distinct from that of macrophages (Guilliams et al., 2014; Hoeffel et al., 2012; Meredith et al., 2012; Satpathy et al., 2012; Schraml et al., 2013). Indeed, DCs develop from a common DC precursor (CDP) (Naik et al., 2007; Onai et al., 2007) via an intermediate cell stage known as the pre-DC (Ginhoux et al., 2009; Liu et al., 2009). In contrast, macrophages develop from embryonic precursors (Ginhoux et al., 2010; Hoeffel et al., 2012; Schulz et al., 2012). Cells that resemble DCs or macrophages can also be derived from monocytes and traditionally have been called monocyte-derived DCs or monocyte-derived macrophages, respectively (Bain et al., 2014; Mildner et al., 2013; Tamoutounour et al., 2013), although it has recently been proposed that they be generically termed monocyte-derived cells (MCs) (Guilliams et al., 2014). Monocytes themselves have been shown to descend from a common monocyte precursor (cMoP) (Hettinger et al., 2013), and both CDPs and cMoPs can be generated from a macrophage-DC progenitor (MDP) population (Fogg et al., 2006; Hettinger et al., 2013; Liu et al., 2009). Thus, one can define classical DCs as cells that descend from CDPs and pre-DCs irrespective of phenotype or function (Guilliams et al., 2014). We have recently provided experimental support for this concept by taking advantage of the fact that CDPs and pre-DCs express DNGR-1 (also known as CLEC9A). We generated *Clec9a*^{cre}*Rosa*^{EYFP} reporter mice in which the *Clec9a* locus control regions drive Cre expression in DNGR-1$^+$ cells, allowing for a recombination event that irreversibly traces CDPs and pre-DCs progeny (Schraml et al., 2013). In these mice, DCs can be reliably identified and distinguished from macrophages and MCs by YFP reporter gene expression (Schraml et al., 2013).

The ontogenetic approach to DC definition has been complemented by identification of core DC and macrophage gene expression signatures that permit reliable separation of the two cell types (Gautier et al., 2012; Miller et al., 2012). This has been made possible by systematic efforts to characterize gene expression profiles of mouse tissue leukocyte populations, notably by the Immgen consortium, and has greatly expanded the

phenotypic method of cell classification (Heng et al., 2008). Global description of gene expression profiles further permits analysis of relationships among leukocytes through unsupervised hierarchical data clustering. Such methodology has offered new insight into the biology of macrophages, MCs, and DCs. For example, it revealed that DCs migrating from peripheral tissues into lymph nodes cluster together independently of tissue of origin, indicating that they adopt a common program of differentiation (Miller et al., 2012). Thus, ontogeny and global gene expression analysis constitute powerful new approaches with which to dissect the heterogeneity of the mononuclear phagocyte system and better define DCs, MCs, and macrophages.

Because of their rarity in tissues, much of the biology of DCs has been surmised from studies of cells grown in vitro from hematopoietic precursors under the influence of growth factors (Caux et al., 1992; Inaba et al., 1992; Naik et al., 2007; Palucka et al., 1998; Sallusto and Lanzavecchia, 1994). In particular, the culture of mouse BM cells with GM-CSF, a cytokine involved in the development and homeostasis of mononuclear phagocytes, has been used extensively to generate $CD11c^+MHCII^+$ cells that resemble tissue DCs and are often termed BMDCs (Inaba et al., 1992; Lutz et al., 1999). The output from GM-CSF cultures is heterogeneous and comprises granulocytes and macrophages in addition to DCs. The latter are reported to be enriched in the loosely adherent culture fraction and to express CD11c and MHCII whereas macrophages are thought to be adherent and negative for CD11c and MHCII (Inaba et al., 1992). As such, many laboratories commonly employ magnetically enriched or FACS-sorted $CD11c^+$ loosely adherent and non-adherent cells as a source of pure BMDCs. Gene expression analysis studies of such cells have assumed that this DC population is homogeneous and that any cell-to-cell variation is the result of different states of DC maturation (Shalek et al., 2013, 2014; Vander Lugt et al., 2014). However, the ontogenetic origin of BMDCs is uncertain and, in fact, $Ly6C^+$ monocytes rather than CDPs have been suggested to act as precursors (Mayer et al., 2014; Xu et al., 2007). As such, it is unclear how GM-CSF-derived BMDCs fit within the recent framework of defining DCs by ontogenetic criteria. Here, we show that $CD11c^+MHCII^+$ cells in BMDC cultures are in fact heterogeneous in terms of hematopoietic origin and gene expression profiles. They encompass at least two distinct populations that derive from either a monocytic or a DC myelopoietic branch and that display distinct immune functions in vitro and in vivo. On the basis of ontogenetic, morphological, and gene expression criteria, we classify these two populations as bona fide DCs and monocyte-derived macrophages. We further show that they both undergo maturation in response to lipopolysaccharide (LPS) yet mount distinct responses to the stimulus and remain separable entities. These findings have implications for the interpretation of numerous studies employing GM-CSF-derived BMDCs as a cell model.

RESULTS

Phenotypic Heterogeneity of GM-CSF-Derived $CD11c^+MHCII^+$ BMDCs

To a variable extent, $CD11c^+MHCII^+$ cells from GM-CSF cultures often present as two sub-populations, one that is believed to represent an immature DC phenotype with intermediate or low expression of MHCII and co-stimulation molecules such as CD40 and CD86 (Figure 1A, blue) and another that has undergone spontaneous maturation and expresses higher amounts of the same markers (Figure 1A, red). However, the transcription factor IRF4 was recently argued to control the development of BMDCs falling within the mature gate, as well as the development of a subset of tissue-resident conventional $CD11b^+$ DCs in mouse small intestine, lung, and spleen (Gao et al., 2013; Persson et al., 2013; Schlitzer et al., 2013; Vander Lugt et al., 2014). It is therefore possible that the heterogeneous phenotype of BMDCs could reflect the presence of different cell subsets rather than, or in addition to, distinct maturation states. Accordingly, $CD11c^+MHCII^{hi}$ mature BMDCs expressed higher amounts of CD24, DEC205, PD-L2, and IRF4 (Figure 1B, red), whereas $CD11c^+MHCII^{int}$ immature BMDCs displayed higher expression of SIRPα, F4/80, and CD11b (Figures 1A and 1B, blue), all markers that can to some extent distinguish subtypes of DCs and macrophages. The mature BMDC subset expressed surface markers generally restricted to DCs (CD135, CCR7, CD117) whereas immature BMDCs expressed higher amounts of markers often associated with monocytes and macrophages (CD64, CD115, CD14) (Figure 1C). In line with these results, *Zbtb46* and *MerTK*, two genes whose expression is argued to mark DCs versus macrophages, respectively (Gautier et al., 2012; Meredith et al., 2012; Miller et al., 2012; Satpathy et al., 2012), were expressed by either the mature or the immature BMDC fractions (Figure 1D). The two BMDC populations could not be distinguished by their differential adhesion to plastic although mature cells were more highly represented in the non-adherent floating cell fraction (Figure 1E). Altogether, these results began to suggest that two types of loosely adherent $CD11c^+MHCII^+$ mononuclear phagocytes might arise in GM-CSF BM cultures, a mature one similar to DCs and an immature one resembling macrophages.

Different Hematopoietic Progenitors Expand in GM-CSF Cultures to Give Rise to $CD11c^+MHCII^+$ Progeny

To further address this issue, we probed the hematopoietic origin of $CD11c^+MHCII^+$ BMDCs. We purified populations of MDPs, CDPs, cMoPs, and monocytes (see Experimental Procedures) from the BM of CD45.2 C57BL/6 mice and co-cultured them with unfractionated BM cells (filler cells) from a CD45.1 congenic strain for 6 days with GM-CSF. The filler cells acted as a source of growth factors and an internal control for BMDC generation (data not shown). Analysis of the $CD45.2^+$ output from the cultures revealed that all precursors were able to expand in GM-CSF cultures and generate $CD11c^+MHCII^+$ cells albeit to a variable extent (Figures 2A and 2B). MDPs and cMoPs expanded vigorously and gave rise to both $MHCII^{hi}CD11b^{int}$ and $MHCII^{int}CD11b^{hi}$ cells (Figures 2A and 2B), which could also be distinguished on the basis of CD24 and SIRPα expression (Figure 2C). The same was true for $Ly6C^{hi}$ and $Ly6C^{lo}$ monocytes although those cells expanded only poorly (Figures 2A and 2B). We could not phenotypically distinguish between $MHCII^{hi}$ $CD11b^{int}$ cells derived from cMoPs versus those developing from $Ly6C^{hi}$ monocytes, suggesting a common developmental pathway (Figure S1). In contrast, CDPs expanded modestly but preferentially gave rise to $MHCII^{hi}CD11b^{int}CD24^{hi}SIRP\alpha^{int}$ cells (Figures 2A–2C). Similarly, when CDPs were purified on the basis

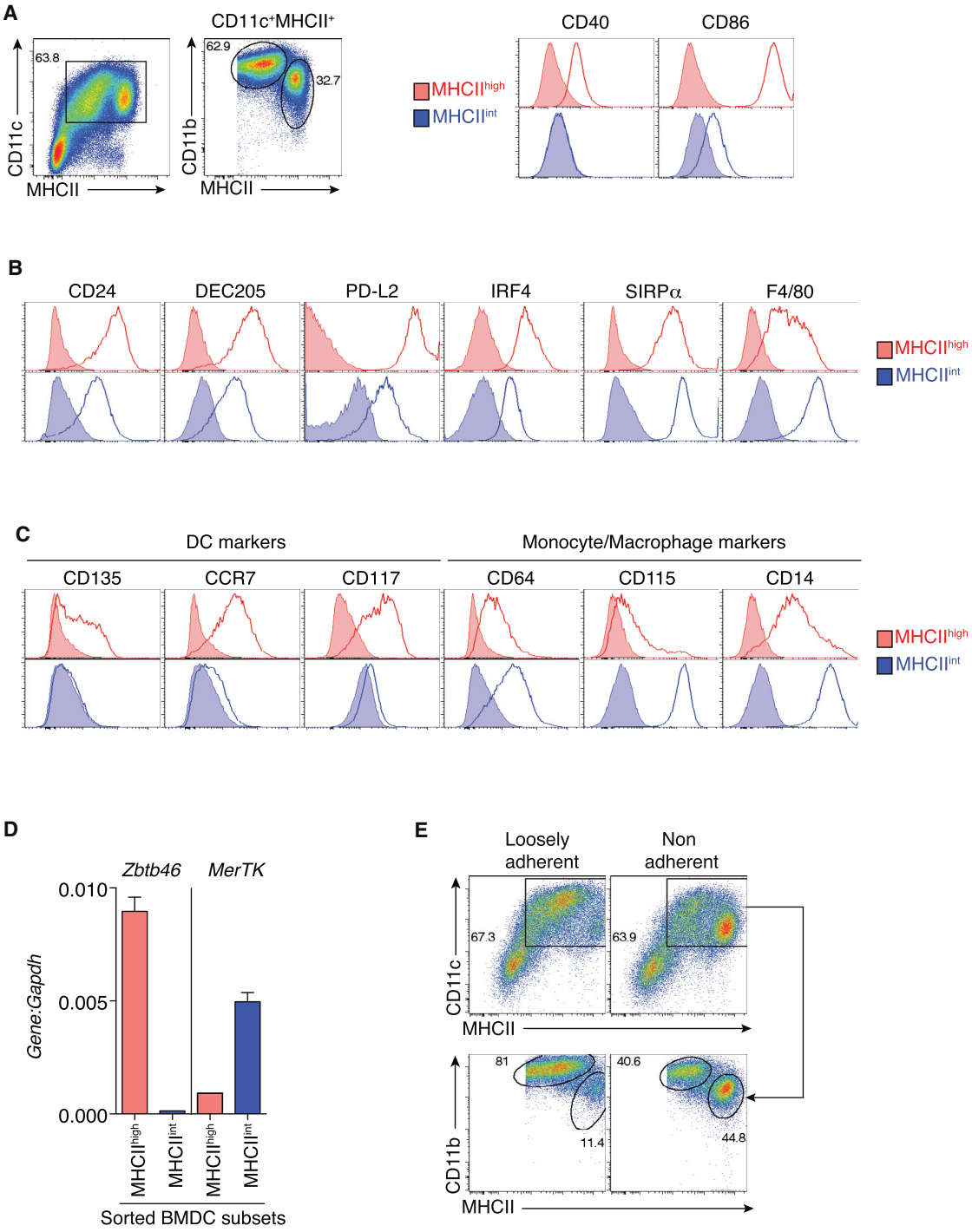

Figure 1. Phenotype of Cells Developing in GM-CSF BM Cultures

(A–C) Phenotype of representative GM-CSF BM cultures at day 6. $CD11c^{+}MHCII^{+}$ BMDCs (A, left) can be sub-divided on the basis of CD11b and MHCII expression (A, right). Boxes depict gates and numbers correspond to percentage of cells in each gate. Histograms showing surface expression of the indicated markers by $MHCII^{hi}CD11b^{lo}$ (red) and $MHCII^{int}CD11b^{hi}$ (blue) subsets. Filled histograms represent isotype-matched irrelevant specificity controls.

(D) Quantitative PCR for *Zbtb46* and *MerTK* transcripts in cDNA from sorted $MHCII^{hi}$ (red) and $MHCII^{int}$ (blue) subsets. Data represent mean ± SD of triplicate wells from one representative experiment.

(E) Flow cytometry analysis of BMDC subsets in loosely adherent versus non-adherent fractions of the GM-CSF culture. Boxes depict gates and numbers correspond to percentage of cells in each gate. Data are representative of at least three experiments.

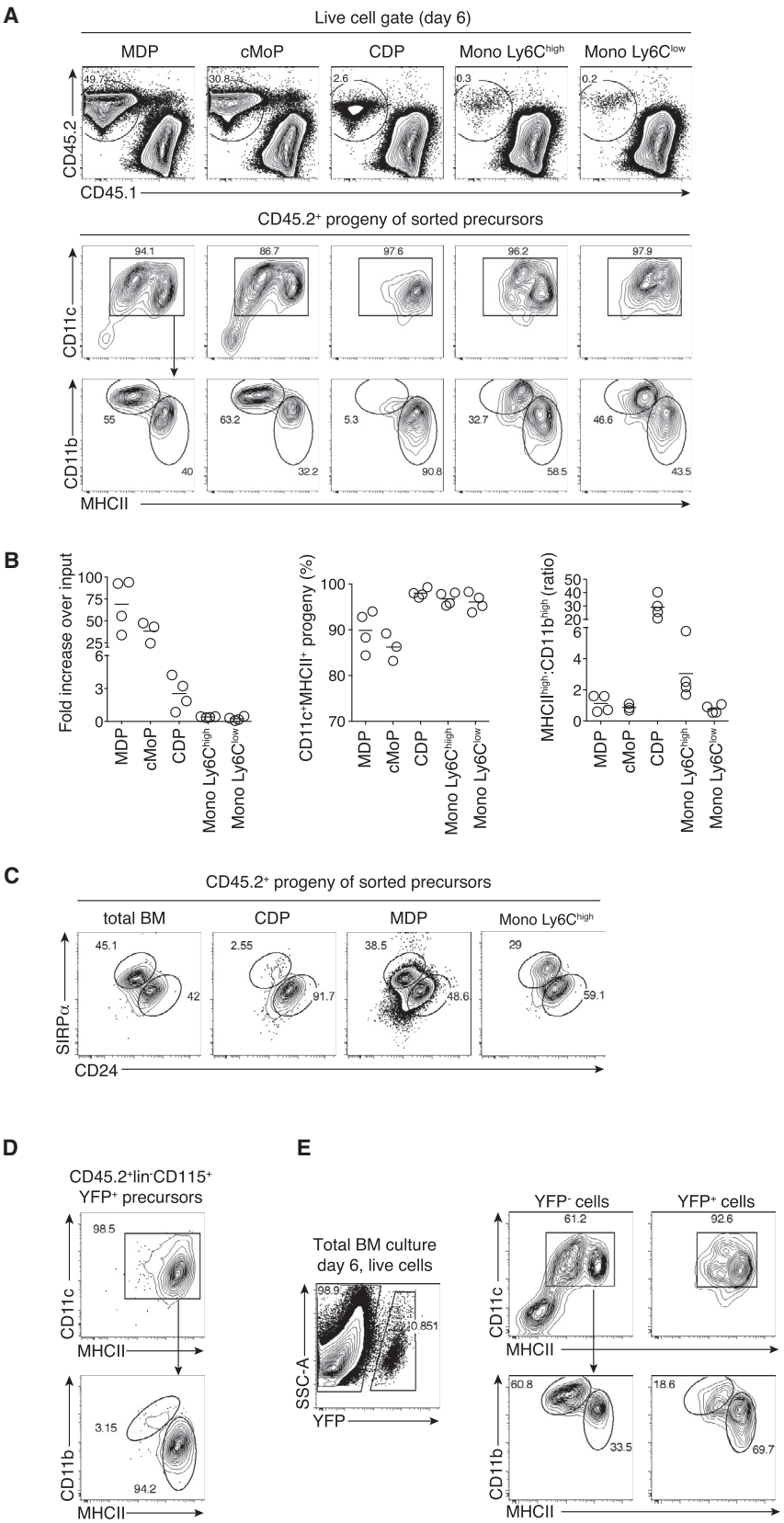

Figure 2. Precursors of Both Monocytes and Dendritic Cells Develop into CD11c$^+$MHCII$^+$ Cells in GM-CSF Cultures

(A) 10^4 of the indicated CD45.2$^+$ progenitors and 10^6 CD45.1 total BM filler cells were co-cultured in the presence of GM-CSF for 6 days. Data show relative proportion of CD45.1 and CD45.2 cells and expression of CD11c, MHCII, and CD11b on CD45.2$^+$ cells before or after gating on CD11c$^+$ MHCII$^+$ cells. Boxes depict gates and numbers correspond to percentage of cells in each gate. Data are representative of four experiments.

(B) Analysis of CD45.2$^+$ cells showing calculated fold-increase in cellularity over input, percentage of CD11c$^+$MHCII$^+$ cells among CD45.2$^+$ cells, and ratio of MHCII^{hi} to CD11b^{hi} cells among CD45.2$^+$ CD11c$^+$MHCII$^+$ cells. Each symbol represents the average of two to three replicates from a single experiment. The bar represents the mean. Four pooled independent experiments are shown.

(C) Analysis of CD24 and SIRPα expression on CD45.2$^+$CD11c$^+$MHCII$^+$ subsets derived from the indicated precursors.

(D) 10^4 CD45.2$^+$ YFP$^+$ cells isolated by cell sorting from the BM of *Clec9a*$^{cre/cre}$*Rosa*$^{WT/EYFP}$ mice were co-cultured for 6 days in GM-CSF with 10^6 CD45.1 total BM filler cells. Data depict flow cytometry analysis of the progeny of CD45.2$^+$ progenitors according to the expression of CD11c, MHCII, and CD11b.

(E) Flow cytometry analysis of YFP, CD11c, MHCII, CD11b expression on day 6 GM-CSF cultures of BM of *Clec9a*$^{cre/cre}$*Rosa*$^{WT/EYFP}$ mice.

In (C)–(E), boxes depict gates, arrows show gating hierarchy, and numbers correspond to percentage of cells in each gate. Data are representative of four experiments. See also Figure S1.

of YFP expression from *Clec9a*$^{cre/cre}$*Rosa*$^{WT/EYFP}$ mice (Schraml et al., 2013), their progeny was exclusively found among CD11c^{+}MHCII^{hi}CD11b^{int} cells (Figure 2D). GM-CSF cultures of total BM cells from the same reporter mice revealed that YFP^{+} progeny of CDPs was highly enriched within the MHCII^{hi} fraction of CD11c^{+} cells, in contrast to YFP^{-} cells, which distributed between CD11c^{-} and CD11c^{+}MHCII^{hi} and CD11c^{+}MHCII^{lo} gates (Figure 2E). Together, these data suggest that the MHCII^{hi} CD11b^{int} population of BMDCs includes both cells derived from CDPs and cells of similar phenotype but derived from cMoPs and monocytes. The MHCII^{int}CD11b^{hi} fraction, in contrast, consists primarily of cells derived from cMoPs and monocytes.

CD11c^{+}MHCII^{+} BMDCs Comprise Cells Resembling Conventional DCs or Macrophages

In an effort to further distinguish cells of different origin, we assessed their expression of CD115 and CD135, receptors for M-CSF and Flt3L, which are necessary for the differentiation of monocyte-derived macrophages and DCs, respectively (Ginhoux et al., 2006, 2009; McKenna et al., 2000; Pixley and Stanley, 2004). CD135^{+} cells were found only among MHCII^{hi}CD11b^{int} cells and could be derived from CDP but not cMoP fractions (Figures 3A and 3B). In contrast, CD115^{+} cells were found in both MHCII^{int}CD11b^{hi} and MHCII^{hi}CD11b^{int} fractions and were primarily derived from cMoPs with only a small contribution from CDPs (Figures 3A and 3B). MDPs gave rise to both CD135^{+} and CD115^{+} cells (Figures 3A and 3B). These results suggest that CD115 and CD135 can be used to identify the two developmentally distinct CD11c^{+}MHCII^{+} mononuclear phagocytes in GM-CSF mouse bone marrow cultures. We therefore designed a gating strategy to purify these subsets from bulk BMDC cultures (Figure 3C). cMoP-derived cells, resembling monocyte-derived macrophages, were defined as CD11c^{+}MHCII^{int}CD115^{+} MerTK^{+} whereas CDP-derived cells, resembling conventional DCs, were defined as CD11c^{+}MHCII^{hi}CD115^{-}CD135^{+} cells (Figure 3C). For the purpose of clarity, we will henceforth refer to these sub-populations as GM-Macs and GM-DCs, respectively, although it should be remembered that both are CD11c^{+}MHCII^{+} and have historically been termed BMDCs.

A large fraction of CD11c^{+}MHCII^{hi} cells from bulk cultures did not express either CD115 or CD135 and were ostensibly neither GM-DCs nor GM-Macs (Figure 3C). When purified by cell sorting and cultured for an extra 3 days in medium with GM-CSF, some of these double-negative cells (GM-DN) upregulated CD135 but not CD115 and became similar to GM-DCs (Figure 3D). However, a proportion of re-cultured GM-DN cells remained CD135 negative, perhaps reflecting those that originated from cMoPs and monocyte precursors (see Figure 3A). In contrast to GM-DN cells, GM-Macs and GM-DCs had a stable phenotype and remained discrete populations even after purification and re-culture for 3 days in GM-CSF medium (Figure 3D). Therefore, we focused subsequent analyses on these populations given their stability and relative homogeneity, although in some but not all settings, we analyzed GM-DN cells in parallel.

Interleukin-4 (IL-4) has sometimes been added to GM-CSF BM cell cultures to generate BMDCs (Lu et al., 1995; Son et al., 2002; Xu et al., 2007). We therefore investigated the phenotype and hematopoietic origin of BMDCs cultured in the presence of both GM-CSF and IL-4. Among CD11c^{+}MHCII^{+} cells arising in GM-CSF + IL-4 culture, two populations could be distinguished using MHCII and CD11b expression (Figure 4A). The MHCII^{int}CD11b^{hi} cells expressed CD115 and MerTK whereas the MHCII^{hi}CD11b^{int} cells did not and some expressed CD135. Similar to GM-CSF-only cultures, all mononuclear phagocyte precursors expanded and differentiated into CD11c^{+} MHCII^{+} cells in GM-CSF + IL-4 cultures. cMoPs expanded to a greater degree than other precursors (Figure 4B). These results suggest that IL-4 does not prevent the development of monocyte-derived macrophages and underscore the notion that CD11c^{+}MHCII^{+} BMDCs are a heterogeneous cell population.

Distinct Functions of GM-Macs and GM-DCs

We compared the behavior of GM-Macs and GM-DCs. GM-Macs had a typical macrophage morphology and were largely immotile (Figure 5A and Movie S1). They produced high amounts of interleukin 6 (IL-6), tumor necrosis factor alpha (TNF-α), chemokine (C-X-C motif) ligand 1 (CXCL1), chemokine (C-C motif) ligand 3 (CCL3), chemokine (C-C motif) ligand 5 (CCL5), and interleukin 12 B subunit (IL-12p40) in response to microbial stimuli (Figure 5B), expressed C-C chemokine receptor type 2 (CCR2, data not shown), and migrated in response to the chemokine (C-C motif) ligand 2, CCL2 (Figure 5C). In contrast, GM-DCs were very motile and continuously extended and retracted dendritic processes (Figure 5A and Movie S2). They produced low amounts of inflammatory cytokines and chemokines in response to microbial stimuli (Figure 5B), expressed C-C chemokine receptor type 7 (CCR7, data not shown), and migrated in response to the CCR7 ligand, chemokine (C-C motif) ligand 21 (CCL21) (Figure 5C). We next analyzed the capacity of each subset to stimulate naive OT-II CD4^{+} T cells specific for the model antigen ovalbumin (OVA). When given pre-processed antigenic peptide, both GM-DCs and GM-Macs displayed comparable ability to stimulate OT-II T cell division and expansion in culture (Figure 5D). The stimulatory ability was not prominently changed by stimulation of the cells with LPS, which is commonly employed to induce DC "maturation" (Figure 5D). In contrast, when given OVA protein, GM-Macs were markedly inferior at stimulating OT-II when compared to GM-DCs, even after LPS stimulation (Figure 5D), despite the fact that they accumulated more antigen by endocytosis (Figure S2). This was most patent at the level of T cell expansion in culture, which was 15-fold lower when GM-Macs rather than GM-DCs were used as antigen-presenting cells (APCs) (Figure 5D). We then examined the ability of either APC subset to stimulate OT-I CD8^{+} T cells in analogous assays. Both GM-DCs and GM-Macs were able to cross-present OVA protein as measured by induction of OT-I proliferation but only T cells primed by GM-DCs upregulated CD25 (Figure 5E). Notably, GM-Macs were less efficient at inducing expression of CD25 in OT-I cells even when given pre-processed OVA peptide and stimulated with LPS (Figure 5E, right). Therefore, the inferior capacity of GM-Macs to stimulate OT-I cells is intrinsic to the cells and not merely attributable to decreased cross-presentation ability. In view of these data, we assessed the ability of each BMDC subset to prime anti-tumor cytotoxic T cells (CTLs) upon infusion into mice. Low numbers of GM-DCs pulsed with OVA peptide were able to induce an anti-OVA CTL response (Figure 5F, left), which was sufficient to protect mice from

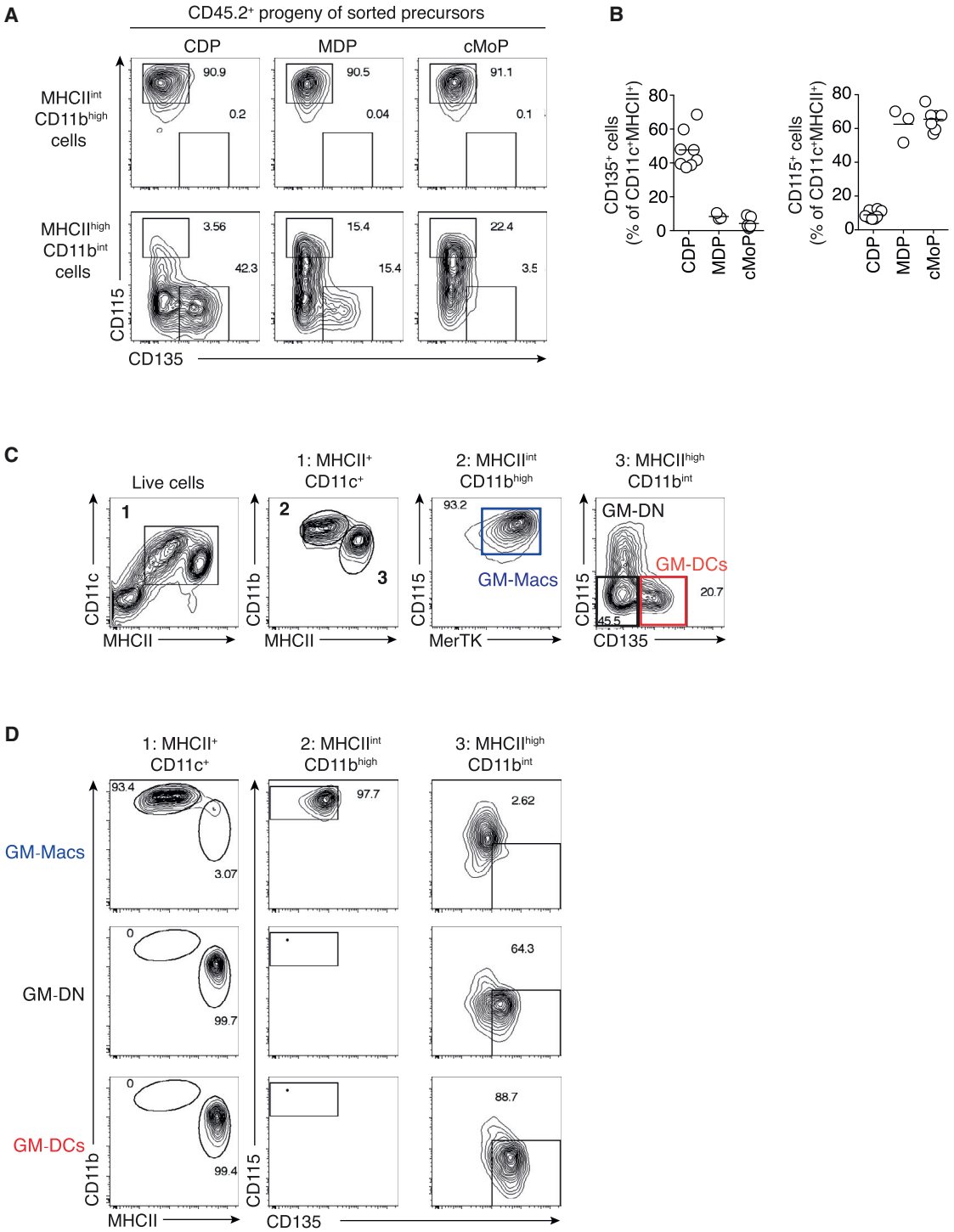

Figure 3. CD11c$^+$MHCII$^+$ BMDCs Comprise Cells Resembling Conventional DCs or Macrophages

(A) CD115 and CD135 expression on CD45.2$^+$CD11c$^+$MHCII$^+$ subsets derived from the indicated precursors and pre-gated as in Figure 2A. Boxes depict gates and numbers correspond to percentage of cells in each gate. Data are representative of three experiments.

(B) Percentage of CD11c$^+$MHCII$^+$ cells expressing either CD115 or CD135 as in (A). Each symbol corresponds to an individual replicate from a pool of four independent experiments. The bar represents the mean.

(C) Flow cytometric definition of GM-DCs, GM-DNs, and GM-Macs from GM-CSF BM cultures. Data depict the total non-adherent and loosely adherent fraction of 6 days GM-CSF BM cultures gated from left to right as indicated.

(D) GM-DCs, GM-DNs, and GM-Macs were FACS sorted at day 6 of GM-CSF BM culture and plated again in 96-well plates with GM-CSF. After 3 days of culture, expression of CD115 and CD135 was measured by flow cytometry. Boxes depict gates and numbers correspond to percentage of cells in each gate. Data are representative of three experiments.

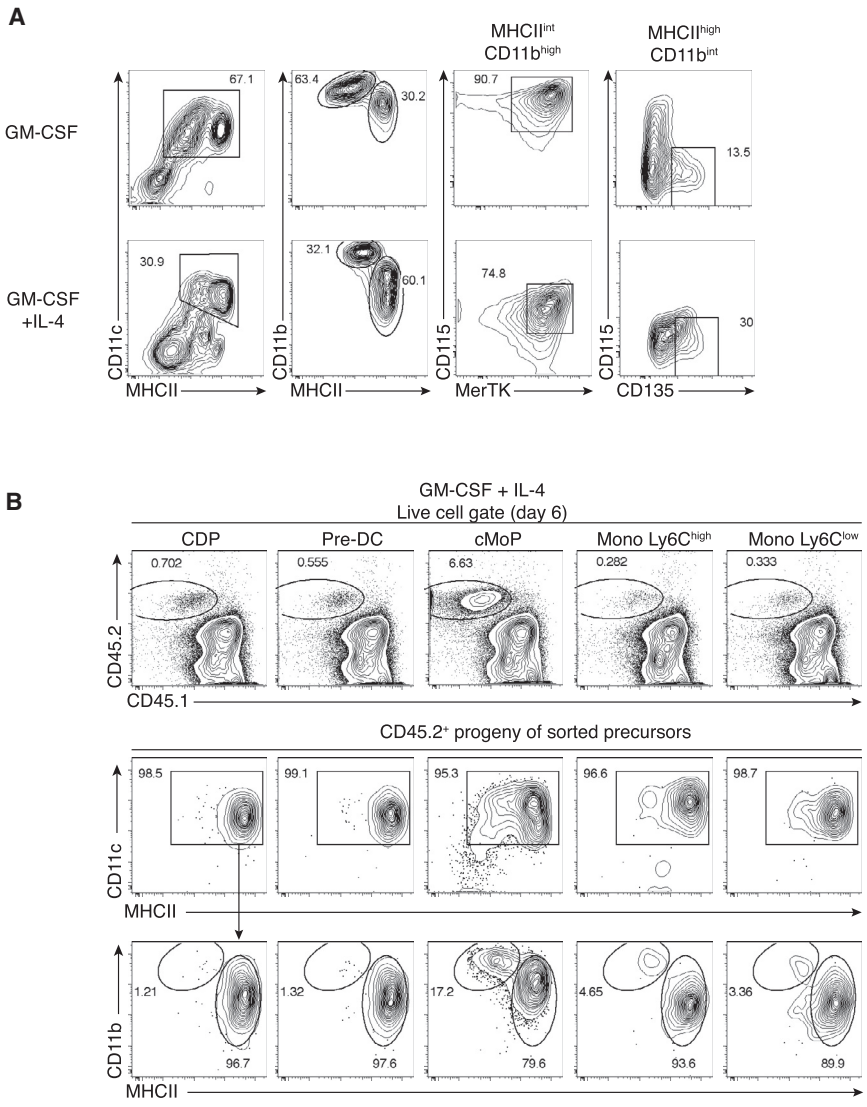

Figure 4. IL-4 Addition Limits but Does Not Prevent Development of Typical GM-Macs

(A) BM cells were cultured with GM-CSF ± IL-4. At day 6, cells were harvested and the expression of CD11c, CD11b, MHCII, CD135, MerTK, and CD115 was analyzed by flow cytometry.

(B) Analysis of the progeny of the indicated CD45.2$^+$ progenitors upon culture in GM-CSF + IL-4. See Figure 2 for experimental details.

Boxes depict gates and numbers correspond to percentage of cells in each gate. Data are representative of three experiments.

subsequent challenge with OVA-expressing B16.F10 melanoma cells (Figure 5F, right). In contrast, around 10-fold higher numbers of GM-Macs were required to elicit the same degree of CTL priming and degree of anti-tumor protection (Figure 5F). The failure of GM-Macs to efficiently induce CTL responses probably reflects their inferior capacity to prime CD8$^+$ T cells coupled to inability to migrate to secondary lymphoid organs in response to CCR7 ligand gradients.

In one series of experiments, we also assessed the functional behavior of GM-DN cells. Despite the fact that they are ontogenetically heterogeneous (see Figures 2 and 3), they were found to resemble GM-DCs, displaying similar morphology (Figure S3A), equivalent capacity to migrate toward CCL21 but not CCL2 (Figure S3B), and corresponding ability to process OVA and efficiently prime CD4$^+$ and CD8$^+$ naive T cells in vitro (Figures S3C and S3D). Altogether, these results indicate that CD11c$^+$MHCII$^+$ BMDCs comprise both motile DCs with superior T cell priming ability and sessile macrophages with marked ability to produce inflammatory mediators in response to innate immune stimuli. The two types of cells display some overlap in phenotype and function, which can be further affected by prior stimulation, for example with LPS.

GM-DC and GM-Macs Express DC and Macrophage Signature Genes

Microarray analysis of CD11c$^+$MHCII$^+$ subsets revealed that macrophage signature genes and a small proportion of DC signature genes are enriched in GM-Macs and the remainder of DC signature genes but not macrophage signature genes are enriched in the GM-DC subset (Figure 6A). Nevertheless, GM-DCs did not uniformly express all the genes that comprise the DC signature. To evaluate the significance of this discrepancy, we analyzed the expression of DC signature genes in four other DC subsets profiled in the Immgen database (Figure S4A). We found that variation in expression of DC signature genes is in fact also seen across DC subsets isolated directly from tissues and is therefore a reflection of natural variation in DC gene expression patterns. Using the DC and macrophage gene signatures, we then performed an unsupervised hierarchical clustering of GM-DCs and GM-Macs with DC and macrophage populations from the Immgen database (Figures S5A and S5B). This confirmed that GM-DCs clustered with DC populations and GM-Macs clustered with macrophage populations. To assess whether maturation overrides these differences and leads to acquisition of a common gene expression signature, we exposed the subsets to LPS. We found that both GM-Macs and GM-DCs behaved similarly with regards to surface expression of CD11c, CD86, and MHCII (Figure 6B) and upregulation of expression of genes characteristic of maturation and LPS response (Figure 6C). Nevertheless, principal-component analysis (PCA) of the expression of all genes revealed that LPS-stimulated GM-Macs clustered with their unstimulated counterparts rather than with GM-DCs (Figure 6D). Likewise, stimulated GM-DCs clustered with unstimulated GM-DCs rather than stimulated GM-Macs (Figure 6D). Similar results were obtained when PCA was restricted to expression of the DC and macrophage core signature genes

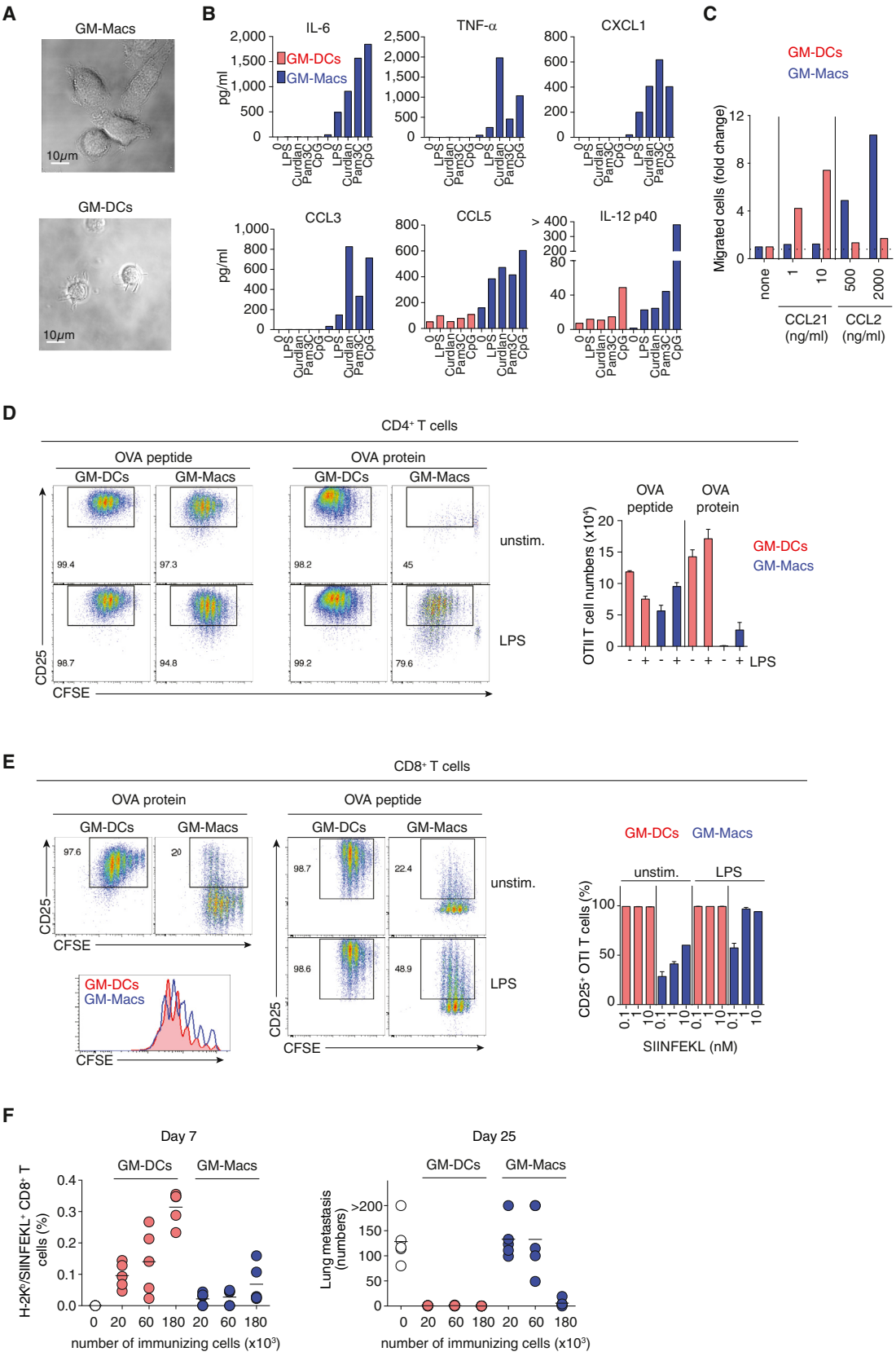

(legend on next page)

(Figures 6E and 6F). These results confirm that GM-Macs and GM-DCs are distinct populations and show that they remain separate entities after undergoing maturation.

To further explore this issue, we performed a Venn diagram analysis and found that GM-DC and GM-Macs display differential responses to LPS with only 794 genes regulated in common and 783 versus 2,469 genes up- or downregulated selectively in GM-DCs versus GM-Macs, respectively (Figure 6G). Among the genes highly expressed in LPS-stimulated GM-DCs were ones encoding typical maturation markers (Figure 6H), which never quite reached the same level of expression in GM-Macs (Figure 6C), despite being greatly upregulated in the latter cells. In contrast, many interferon-stimulated genes were more highly expressed in LPS-stimulated GM-Macs than in GM-DCs (Figure 6H).

In Vivo Equivalence of GM-DCs and GM-Macs

Finally, we analyzed the gene expression patterns of unstimulated and LPS-stimulated GM-DCs and GM-Macs to identify their closest relatives in vivo by reference to the Immgen database. We first performed unsupervised hierarchical clustering of the transcriptome of GM-DCs and that of DCs isolated from various organs (Figure 7A). We found that GM-DCs, although distinct from all other DC types, clustered most closely with migratory DCs (Miller et al., 2012) (Figure 7A) and expressed many migratory DC signature genes (Figure 7B), as recently suggested for "mature BMDCs" generated with GM-CSF and IL-4 (Vander Lugt et al., 2014). Accordingly, GM-DCs might constitute a useful in vitro model to study the properties of migratory DCs. To evaluate the relationship between GM-DCs and the two major classical DC subsets, we analyzed the expression of genes specific to the CD8α^+ and CD8α^- DC families (Balan et al., 2014; Mayer et al., 2014). GM-DCs did not appear to belong to either DC subset (Figure S6). However, their development appears to be controlled by IRF4 (Gao et al., 2013), so GM-DCs might be more closely related to the CD8α^- DC family, perhaps consistent with their expression of CD11b and SIRPα.

We then performed the same unsupervised hierarchical clustering for GM-Macs. GM-Macs clustered separately from other macrophages, with their closest relatives being alveolar macrophages, splenic red pulp macrophages, and peritoneal macrophages (Figure 7C). Consistent with that notion, GM-Macs expressed some of the genes also found in those three populations (Figure 7D). Because those macrophage populations are derived from embryonic precursors whereas GM-Macs originate from monocytes, we separately evaluated the relationship of the GM-Macs to monocytes, monocyte-derived DCs, and monocyte-derived macrophages found in the dermis (McGovern et al., 2014; Tamoutounour et al., 2013). We found that GM-Macs clustered together with both dermal monocyte-derived DCs and macrophages, separately from blood or extravasated Ly6C^{hi} monocytes (Figure S7). However, GM-Macs occupied a branch of their own, distinct from all recently described dermal monocyte-derived cell subtypes. The fact that GM-Macs do not correspond to a known macrophage population probably reflects recent findings that the identity of macrophages is largely imprinted by the microenvironment irrespective of monocytic or embryonic origin (Gosselin et al., 2014; Lavin et al., 2014). Macrophages grown in culture are therefore unlikely to ever mimic any one tissue macrophage subtype. We conclude that GM-DCs and GM-Macs are discrete in-vitro-generated populations of mononuclear phagocytes that resemble but are distinct from DCs and macrophages found in vivo.

DISCUSSION

GM-CSF-derived BMDCs have been used as a model to study DC biology in countless studies. Although the cellular heterogeneity in GM-CSF cultures has been appreciated from the beginning (Inaba et al., 1992), it has generally been thought that non-DCs can be eliminated by early washing steps, discarding highly adherent cells and enriching or sorting for CD11c$^+$ cells. With some exceptions (Gao et al., 2013), the underlying assumption has been that the CD11c$^+$ cells obtained in this manner constitute pure DC populations and that any heterogeneity in phenotype and function is a result of "spontaneous" maturation of the cells in culture (Gallucci et al., 1999; Jiang et al., 2007). Here, we demonstrate that this assumption is incorrect and that the CD11c$^+$MHCII$^+$ fraction of GM-CSF cultures comprises at least two cell types that by ontogenetic and gene expression criteria correspond to monocyte-derived macrophages and CDP-derived DCs. Notably, both undergo maturation in response to LPS but respond differentially to the stimulus and display distinct functional properties. This hitherto unappreciated heterogeneity of CD11c$^+$MHCII$^+$ cells from GM-CSF bone marrow cultures complicates the interpretation of studies that

Figure 5. GM-DCs and GM-Macs Have Distinct Phenotype and Function

(A) Morphology of GM-DCs and GM-Macs. See also Movies S1 and S2.

(B) GM-DCs and GM-Macs were cultured with the indicated stimuli. Accumulation of inflammatory cytokines and chemokines in the supernatant was measured after 24 hr.

(C) Differential response of GM-DCs and GM-Macs to CCR7 and CCR2 agonists. Chemotaxis to CCL2 and CCL21 was measured over a 2 hr period.

(D) Stimulation of CD4$^+$ T cells. GM-DCs and GM-Macs were incubated with OVA protein or OVA$_{323-339}$ peptide with or without LPS and co-cultured with CFSE-labeled naive CD4$^+$ OT-II T cells. T cell proliferation and expansion were assessed after 5 days. Data in the bar graph are mean ± SD of triplicate wells for the representative experiment shown on the left.

(E) Left: GM-DCs and GM-Macs were incubated with OVA protein and co-cultured with CFSE-labeled naive CD8$^+$ OT-I T cells. T cell proliferation and activation were assessed by flow cytometry after 3 days. Right: GM-DCs and GM-Macs were incubated with or without LPS followed by pulsing with OVA$_{257-264}$ peptide, washing, and co-culturing with CFSE-labeled naive CD8$^+$ OT-I T cells. T cell proliferation and activation were assessed by flow cytometry after 3 days. Data in the bar graph are mean ± SD of triplicate wells for the representative experiment shown at left. Dot plots are for data obtained with APCs pulsed with 0.1 nM peptide.

(F) The indicated number of GM-DCs and GM-Macs were pulsed with OVA$_{257-264}$ peptide and infused intravenously into mice, which were then challenged with B16-OVA tumor cells. Data depict frequency of OVA-specific CD8$^+$ T cells in blood and rejection of B16-OVA lung pseudo-metastases. The bar represents the mean.

Data are representative of two to three experiments. See also Figures S2 and S3.

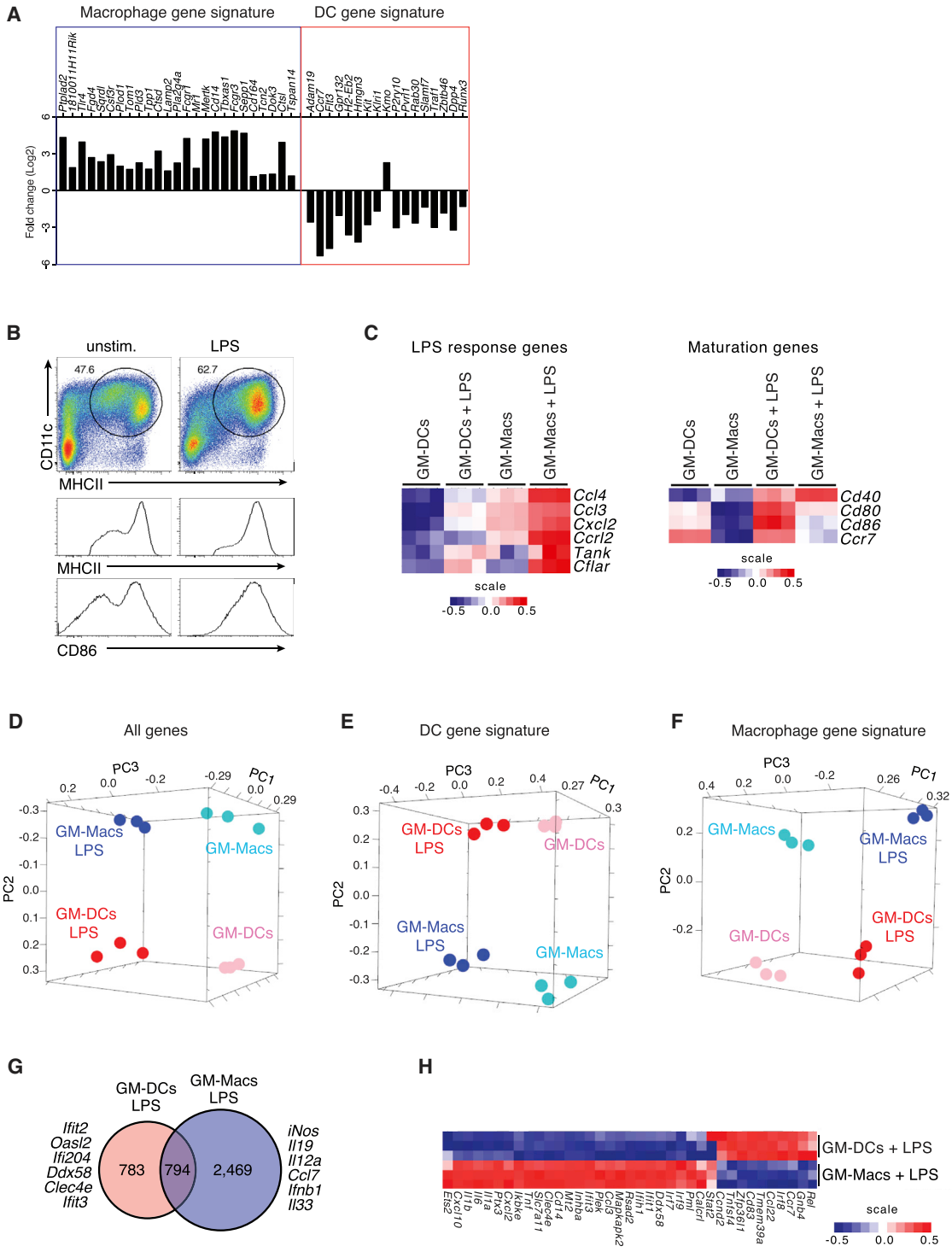

Figure 6. LPS Stimulation Does Not Lead to Convergence of Gene Expression Profiles of GM-DCs and GM-Macs

(A) Expression of transcripts corresponding to the Immgen signatures for macrophages and DCs. Data are expressed as a log2 difference of expression in GM-Macs relative to GM-DCs and are the average of triplicate samples.

(B) Total GM-CSF BM cultures were given no stimulus or 100 ng/ml of LPS overnight. Expression of select maturation markers was analyzed by flow cytometry.

(C) Heat map of gene expression for select LPS-responsive genes and markers of maturation, comparing unstimulated or LPS-stimulated sorted GM-Macs and GM-DCs populations. Individual replicates are shown.

(D) Principal-component analysis of all genes expressed in GM-Macs and GM-DCs stimulated or not with 10 ng/ml of LPS for 4 hr. Each dot of the same color corresponds to a replicate sample.

(legend continued on next page)

have rested on the assumption that they represent a single cell type.

Although the ontogeny of BMDCs has not, until now, been systematically dissected, it has often been suspected that GM-CSF-derived BMDCs might be of monocytic origin based on the analysis of the expansion of Ly6C$^+$ monocytes in GM-CSF cultures (Mayer et al., 2014; Sallusto and Lanzavecchia, 1994; Xu et al., 2007). Moreover, because GM-CSF in some in vivo settings of inflammation triggers the differentiation of monocytes into CD11c$^+$MHCII$^+$ cells (Naik et al., 2006), it has been thought that GM-CSF-derived BMDCs might be the in vitro equivalent of ''monocyte-derived DCs,'' elicited in vivo by infection or inflammation (Serbina et al., 2003). Here, we confirm that monocyte-committed precursors expand vigorously in culture and can give rise to CD11c$^+$MHCII^{hi} cells. However, we also show that the latter can arise from the expansion and differentiation of DC-restricted precursors. These results highlight a previously unappreciated ability of CDPs to expand in GM-CSF cultures and give rise to cells that express CD135, which we term GM-DCs and constitute bona fide DCs by ontogenetic criteria.

The frequency of GM-DCs and GM-Macs in GM-CSF cultures is likely to vary from laboratory to laboratory or even, over time, within a single laboratory based on such factors as variations in culture medium, batch of fetal calf serum, batch and concentration of GM-CSF, tissue culture plastic, or experimental technique. For example, some investigators dispense with the original step of washing away non-adherent cells (Lutz et al., 1999), and others utilize IL-4 in addition to GM-CSF or employ different culture lengths, which might differentially affect output from different progenitors that require growth factors produced by other cells developing within the culture. It is therefore possible that some investigators have historically used cultures from which GM-Macs are largely absent. On the other hand, others have reported a very high proportion of CD11c$^+$ cells that express CD115 and CD14 in GM-CSF cultures, which probably corresponds to the GM-Macs characterized here (Mayer et al., 2014). Once one accepts that CD11c$^+$MHCII$^+$ BMDCs might be heterogeneous, it becomes important to ensure that this does not impact experimental conclusions. In this regard, our finding that LPS-driven induction of maturation genes is greater in GM-DCs while that of interferon-stimulated genes is higher in GM-Macs bears on the interpretation of recent analysis of the expression of the same sets of genes after single-cell RNA sequencing of LPS-stimulated BMDCs (Shalek et al., 2013). In retrospect, the notable cell-to-cell variations in DC responses to stimulation found in those studies (Shalek et al., 2013, 2014) might be in part attributable to differential sampling and sequencing of GM-DCs versus GM-Macs. It might therefore be safer to employ DC culture methods that rely on Flt3L-dependent differentiation of CDPs and preDCs (Naik et al., 2007), although those can also lead to the growth of CD115$^+$ cells that might constitute monocyte progeny (Mayer et al., 2014).

In addition to the CD135$^+$ and CD115$^+$ cells that we define as GM-DCs and GM-Macs, respectively, the CD11c$^+$MHCII$^+$ fraction of GM-CSF cultures comprises a large fraction of ''DN'' cells that do not express CD115 or CD135. Our precursor differentiation analysis suggests that GM-DN cells are ontogenetically heterogeneous. Nevertheless, they present similar functional properties to GM-DCs and it is interesting to note that they generate a large proportion of CD135$^+$ GM-DCs upon re-culture. It is therefore tempting to conclude that DN cells predominantly comprise a population of GM-DCs that are at an earlier stage of differentiation and derive from CDPs. If this is the case, for experimental purposes, it might be sufficient to discriminate CD11c$^+$ MHCII$^+$ BMDCs on the basis of CD115 expression, increasing GM-DC yield and simplifying purification. Yet, it is important to note that cMoP and monocyte progeny can nevertheless be found in the DN gate. Therefore, when maximum homogeneity is desired, we would advocate including CD135 expression as an additional stringency criterion to identify GM-DCs.

In summary, we demonstrate a previously unappreciated heterogeneity in CD11c$^+$MHCII$^+$ GM-CSF-derived ''BMDCs'' and show that some features of DC maturation might equally apply to certain types of macrophages. In this regard, it will be important to assess in further studies whether macrophages might stimulate certain types of T cell response in some instances (Gao et al., 2013). Our data add to the notion that traditional approaches to define mononuclear phagocyte populations based on phenotype and function need to be revised to take into account ontogeny and gene expression patterns. Refinement of in vitro DC culture systems will inevitably lead to a better understanding of the function of DCs and macrophages and has implications for the design of cell-based vaccines for use in humans.

EXPERIMENTAL PROCEDURES

Mice

C57BL/6J, B6.SJL, *Clec9a*$^{cre/cre}$*Rosa*$^{WT/EYFP}$, OT-I × *Rag1*$^{-/-}$, and OT-II mice were bred at the London Research Institute in specific-pathogen-free conditions. All experiments were performed in accordance with national and institutional guidelines for animal care and were approved by the London Research Institute Animal Ethics Committee and by the Home Office, UK.

GM-CSF Cultures

10 × 10^6 bone marrow cells per well were cultured in tissue-culture-treated 6-well plates in 4 ml of complete medium (RPMI 1640 supplemented with glutamine, penicillin, streptomycin, 2-mercaptoethanol [all from Invitrogen]), 10% heat-inactivated fetal calf serum (Source BioScience), and GM-CSF (20 ng/ml, Peprotech). Half of the medium was removed at day 2 and new medium supplemented with GM-CSF (2×, 40 ng/ml) and warmed at 37°C was added. The culture medium was entirely discarded at day 3 and replaced by fresh warmed medium with GM-CSF (20 ng/ml). For some experiments, 5 ng/ml of IL-4 (Peprotech) was added together with GM-CSF and maintained

(E) Same as (D) but analyzing only DC signature genes (Immgen).
(F) Same as (D) but analyzing only macrophage signature genes (Immgen).
(G) Venn diagram of genes differentially up- or downregulated by GM-Macs or GM-DCs in response to LPS, averaged from triplicate samples. Number of genes in each region is indicated and examples of genes uniquely induced by LPS in GM-Macs or GM-DCs are shown.
(H) Heat map of selected transcripts in three independent samples of LPS-stimulated GM-Macs and GM-DCs. Data are pooled from three independent experiments.
See also Figures S4–S7.

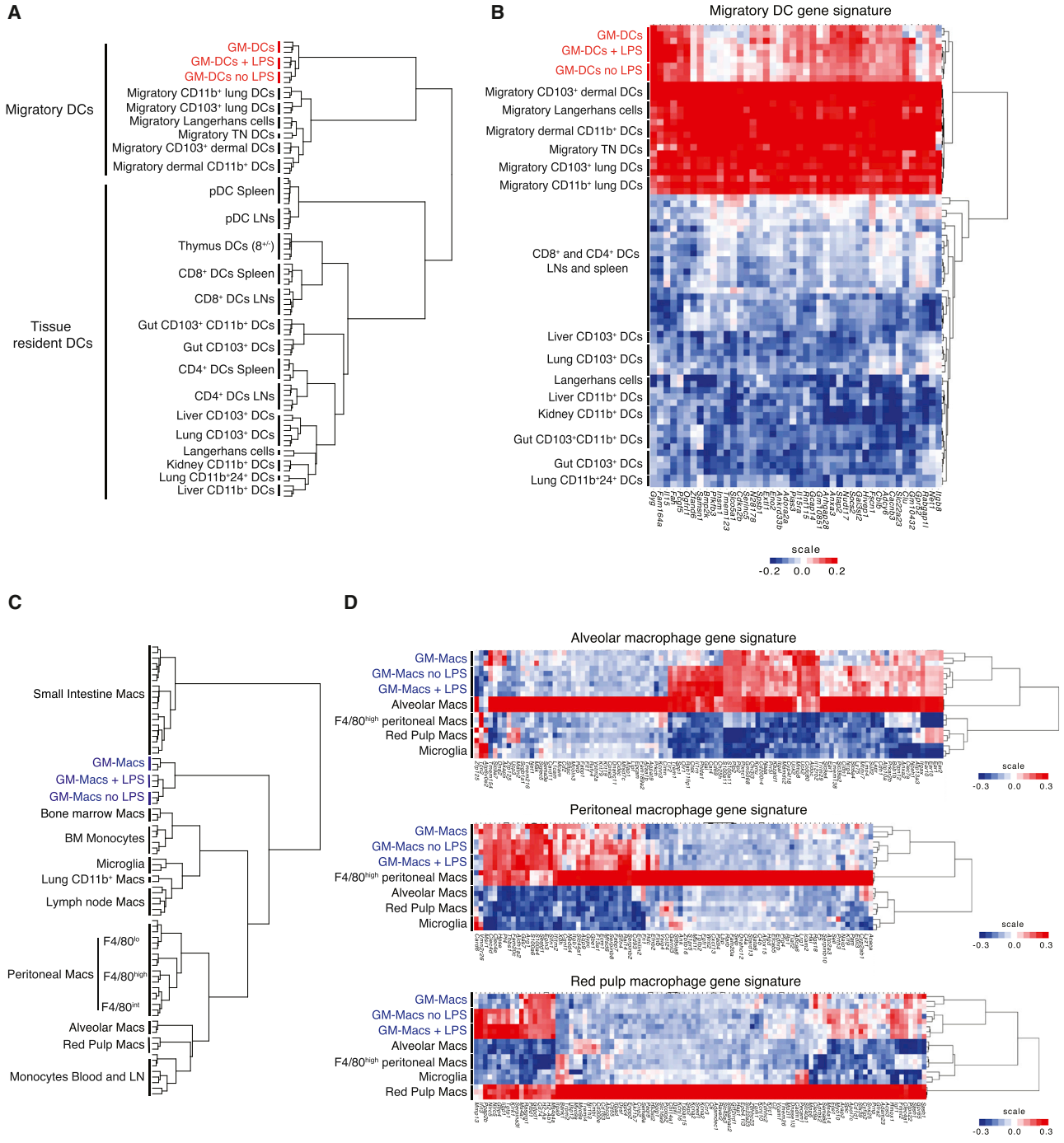

Figure 7. Correlation of GM-DCs and GM-Macs to In Vivo Mononuclear Phagocyte Subsets

(A) Hierarchical clustering of triplicate samples of unstimulated (freshly sorted [GM-DCs] or subsequently cultured without LPS [GM-DCs no LPS]) or LPS-stimulated GM-DCs (GM-DCs + LPS) and replicates of DC subsets deposited in the Immgen database. The 20% of genes with the most variable expression were used for the analysis.

(B) Population clustering and heat map of relative transcript value for migratory DC signature genes in unstimulated (freshly sorted [GM-DCs] or subsequently cultured without LPS [GM-DCs no LPS]) or LPS-stimulated GM-DCs (GM-DCs + LPS) compared to murine DC populations from the Immgen database.

(C) Hierarchical clustering of triplicate samples of unstimulated (freshly sorted [GM-DCs] or subsequently cultured without LPS [GM-DCs no LPS]) or LPS-stimulated GM-Macs (GM-Macs + LPS) and replicates of macrophage subsets deposited in the Immgen database. The 20% of genes with the most variable expression were used for the analysis.

(D) Population clustering and heat map of relative transcript value for alveolar, peritoneal, or red pulp splenic macrophage signature genes in unstimulated (freshly sorted [GM-DCs] or subsequently cultured without LPS [GM-DCs no LPS]) or LPS-stimulated GM-Macs (GM-Macs + LPS) compared to murine macrophage populations from the Immgen database. Data are pooled from three independent experiments.

at that concentration throughout medium changes. On day 6, non-adherent cells in the culture supernatant and loosely adherent cells harvested by gentle washing with PBS were pooled and used as the starting source of material for most experiments.

Flow Cytometry Analysis

Cells were stained in ice-cold PBS containing FCS (2%) and EDTA (2 mM) using appropriate antibody-fluorophore conjugates. Multiparameter analysis was performed on a Fortessa analyzer (BD Biosciences) and analyzed with FlowJo software (Tree Star). The following antibodies were purchased from BD Bioscience: anti-CD8α (clone 53-6.8), anti-Ly6c (clone AL-21), anti-CD49b/Pan-NK cells (clone DX5), anti-CD45.1 (clone A20), anti-CD3ε (clone 145-2C11), anti-CD4 (clone RMA4.5), anti-CD16/32 (clone 2.4G2; Fc block), anti-B220 (clone RA3-6B2), anti-CD40 (clone 3/23), anti-SIRPα (clone P84), anti-CD25 (clone PC61), anti-CD24 (clone M1/69), and anti-CD62L (clone MEL-14). The following antibodies were purchased from Biolegend: anti-F4/80 (clone C1:A3-1), CD11c (clone N418), anti-CD64 (clone X5-4/7.1), anti-CD86 (GL-1), anti-Gr-1 (clone RB-8C5), anti-CD117 (clone 2B8), anti-CD135 (clone A2F10), anti-CD205 (clone NLDC-145), anti-Ter119 (clone TER119), and anti-CD64 (clone X54-5/7.1). The following antibodies were purchased from eBioscience: anti-CD45.1 (clone A20), anti-CD45.2 (clone 104), anti-MHCII I-A/I-E (clone M5/114.15.2), anti-CD11b (cloneM1/70), anti-Ly6G (clone RB6-8C5), anti-CD115 (clone AFS98), anti-CD44 (clone IM7), anti-PDL2 (clone TY25), anti-IRF4 (clone 3E4), anti-CD14 (clone Sa2-8), and anti-CCR7 (clone 4B12). Anti-MerTK (BAF591) was purchased from R&D System. Anti-DNGR-1 (clone 1F6) (Sancho et al., 2008) was produced in-house. Corresponding isotype-matched irrelevant specificity controls were purchased from BD, Biolegend, and eBioscience. H-2K^b/SIINFEKL pentamers were purchased from Proimmune. Prior to acquisition, cells were resuspended in PBS/FCS 2%/EDTA (2 mM) solution with 1 μg/ml of DAPI to exclude dead cells. Live cell counts were calculated from the acquisition of a fixed number of 10-μm latex beads (Beckman Coulter) mixed with a known volume of unstained cell suspension. For intracellular staining, cells were fixed and permeabilized using the CytoFix/Cytoperm kit (BD).

Cell Sorting

Cells were sorted on a BD FACS Aria (BD Biosciences). For sorting of progenitors, total BM cells were isolated and lineage-negative cells were enriched using magnetic beads. In brief, cells were incubated with Fc-block (BD Biosciences) for 10 min, stained with biotin conjugated antibodies against lineage markers (see below), and washed before incubation with anti-biotin beads and enrichment on LD columns (both Miltenyi Biotec). The flow-through fraction was stained with antibodies (see below) and FACS sorted to achieve 99% purity. Dead cells were excluded via DAPI.

Lineage markers for MDPs, cMoPs, and CDPs were CD8, CD4, B220, CD19, DX5, Ter119, Ly6G, CD11c, and MHCII. Gating criteria were as follows: for MDPs: Lin$^-$, CD115$^+$, CD117^{hi}, CD135$^+$, DNGR-1$^-$, Ly6C$^-$, CD11b$^-$; for cMoPs: Lin$^-$, CD115$^+$, CD117^{hi}, Ly6C$^+$, CD11b$^-$, CD135$^-$, DNGR-1$^-$; for CDPs: Lin$^-$, CD115$^+$, DNGR-1$^+$, CD117^{lo}; and for CDPs from *Clec9a*$^{cre/cre}$*Rosa*$^{WT/EYFP}$ mice: Lin$^-$, YFP$^+$.

Lineage markers for monocytes were CD8, CD4, B220, CD19, DX5, Ter119, and Ly6G. Gating criteria were as follows: for monocytes Ly6C$^+$: Lin$^-$, CD115$^+$, CD11b$^+$, Ly6C$^+$, CD117$^-$, DNGR-1$^-$; for monocytes Ly6C-: Lin$^-$, CD115$^+$, CD11b$^+$, Ly6C$^-$, CD117$^-$, DNGR-1$^-$.

For sorting GM-DCs and GM-Macs, cultures pooled from at least three mice were harvested at day 6 and stained with anti-MHCII, -CD11c, -CD11b, -CD135, -CD115, -MerTK and sorted according to the gating strategy depicted in Figure 3C. Dead cells were excluded via DAPI.

In Vitro T Cell Assays

OT-II T Cells

CD4$^+$ T cells from spleens and lymph nodes of OT-II mice were enriched by magnetic separation using Dynal mouse CD4 negative isolation kit, according to manufacturer's instructions. Enriched CD4$^+$ T cells were then stained with anti-CD4, anti-CD44, and anti-CD62L antibodies and naive OT-II cells were FACS sorted to achieve 99% purity (CD4$^+$CD44$^-$CD62L$^+$). Sorted cells were labeled with CFSE at 37°C for 10 min, washed, and counted before culture with APCs.

OT-I T Cells

CD8$^+$ T cells from spleens and lymph nodes of OT-I × *Rag1*$^{-/-}$ mice were purified from single-cell suspension by magnetic separation on LS columns (Miltenyi) after labeling with PE-conjugated anti-CD8 antibody and anti-PE microbeads (Miltenyi) according to the manufacturer's instructions. Enriched cells were labeled with CFSE at 37°C for 10 min, washed, and counted before culture with APCs.

Stimulation

Sorted GM-DCs, GM-DN cells, or GM-Macs (gating strategy in Figure 3C) were incubated in 96-well round-bottom tissue culture plates. For OT-II stimulation, GM-DCs, GM-DN cells, or GM-Macs were incubated with endotoxin-free OVA protein (10 or 20 μg/ml) or OVA$_{323-339}$ peptide (10 μM) in the presence or absence of 100 ng/ml of LPS and co-cultured with naive CFSE-labeled OT-II T cell. For OT-I stimulation, GM-DCs, GM-DN cells, and GM-Macs were incubated with endotoxin-free OVA protein (150 μg/ml) or were pre-treated or not with 10 ng/ml of LPS for 2 hr and pulsed for 20 min with various concentrations of OVA$_{257-264}$ peptide (0.1, 1, or 10 nM) before washing. 50,000 GM-DCs, GM-DN cells, or GM-Macs were incubated with 50,000 T cells. T cell proliferation and activation was assessed by flow cytometry after 3 days for OT-I T cells and after 5 days for OT-II T cells.

To assess OVA uptake, total non-adherent and loosely adherent cells from GM-CSF cultures were collected at day 6 and 10^5 cells were plated in 96-well round-bottom plates. The next day, cells were incubated at 4°C or 37°C with OVA-Alexa647 (Molecular Probes) for 1 hr. Cells were then stained with anti-CD11c, -MHCII, -CD11b, -CD115, -MerTK, -CD135 and presence of Alexa647 signal was analyzed by flow cytometry in GM-DCs or GM-Macs identified according to the strategy depicted in Figure 3C.

In Vivo CTL Priming

Sorted GM-DCs and GM-Macs (gating strategy Figure 3C) were incubated in complete RPMI-1640 medium with 100 nM of OVA$_{257-264}$ peptide for 30 min. Cells were washed extensively in PBS and injected intravenously into the tail vein of C57BL/6 mice. H-2K^b/SIINFEKL MHC pentamers were used for the detection of OVA-specific CD8$^+$ T cells in the blood 7 days after immunization. On the same day (day 7), mice were challenged intravenously with OVA-expressing B16 melanoma cells (2.5 × 10^5 mouse). Mice were sacrificed 18 days after tumor challenge (day 25) and tumor burden was assessed by counting lung foci.

Microarrays and Gene Expression Analysis

GM-DCs and GM-Macs were sorted according to the gating strategy depicted in Figure 3C to achieve 99% purity. For LPS stimulation, sorted GM-DCs and GM-Macs were cultured with or without 10 ng/ml of LPS for 4 hr in complete medium, before further processing. For each population, total RNA was extracted with RNeasy Micro- or Minikit (QIAGEN). RNA was hybridized on the Affymetrix Mouse Gene 1.0 ST array according to the manufacturer's instructions. Each analysis was performed in triplicate using independently sorted cells prepared from independent cultures, each started with BM pooled from at least three mice. Data were analyzed with Bioconductor 2.13 (http://www.bioconductor.org) running on R 3.0.2 (available from http://www.R-project.org). Probeset expression measures were calculated with the Affymetrix package's Robust Multichip Average (RMA) default method. Differentially expressed genes were assessed between samples using an empirical Bayes t test (limma package). p values were adjusted for multiple testing by the Benjamini-Hochberg method. Any probe sets that exhibited an adjusted p value of 0.05 were called differentially expressed. Two-dimensional hierarchical clustering of expression data using DC and macrophage signature genes obtained from Immgen (Gautier et al., 2012; Miller et al., 2012) was carried out using a 1 − Pearson correlation distance matrix and average linkage clustering. Genes were clustered using a Euclidean distance matrix. For heat map analysis, colors indicate the expression value relative to the mean expression value per gene in the dataset. Red indicates upregulation and blue indicates downregulation relative to mean value.

ACCESSION NUMBERS

The accession numbers for the microarray data reported in this paper are GEO: GSE62361 and GSE62746. Microarray data from previous studies that

are used for comparative analysis in this paper are available under the accession number GEO: GSE49358 and from the Immgen database (http://www.immgen.org).

SUPPLEMENTAL INFORMATION

Supplemental Information includes Supplemental Experimental Procedures, seven figures, and two movies and can be found with this article online at http://dx.doi.org/10.1016/j.immuni.2015.05.018.

AUTHOR CONTRIBUTIONS

J. Helft and C.R.S. designed the study, analyzed data, and wrote the manuscript. J. Helft, with assistance from J.B., J. Huotari, S.Z., and B.U.S., conducted experiments. P.C. and J. Helft carried out bioinformatic analysis.

ACKNOWLEDGMENTS

We thank the LRI FACS laboratory for technical help. We are grateful to all members of the Immunobiology laboratory for helpful discussions and comments. This work was supported by the ERC and core funding from Cancer Research UK.

Received: December 16, 2014
Revised: March 4, 2015
Accepted: March 31, 2015
Published: June 16, 2015

REFERENCES

Bain, C.C., Bravo-Blas, A., Scott, C.L., Gomez Perdiguero, E., Geissmann, F., Henri, S., Malissen, B., Osborne, L.C., Artis, D., and Mowat, A.M. (2014). Constant replenishment from circulating monocytes maintains the macrophage pool in the intestine of adult mice. Nat. Immunol. *15*, 929–937.

Balan, S., Ollion, V., Colletti, N., Chelbi, R., Montanana-Sanchis, F., Liu, H., Vu Manh, T.P., Sanchez, C., Savoret, J., Perrot, I., et al. (2014). Human XCR1+ dendritic cells derived in vitro from CD34+ progenitors closely resemble blood dendritic cells, including their adjuvant responsiveness, contrary to monocyte-derived dendritic cells. J. Immunol. *193*, 1622–1635.

Banchereau, J., and Steinman, R.M. (1998). Dendritic cells and the control of immunity. Nature *392*, 245–252.

Caux, C., Dezutter-Dambuyant, C., Schmitt, D., and Banchereau, J. (1992). GM-CSF and TNF-alpha cooperate in the generation of dendritic Langerhans cells. Nature *360*, 258–261.

Fogg, D.K., Sibon, C., Miled, C., Jung, S., Aucouturier, P., Littman, D.R., Cumano, A., and Geissmann, F. (2006). A clonogenic bone marrow progenitor specific for macrophages and dendritic cells. Science *311*, 83–87.

Gallucci, S., Lolkema, M., and Matzinger, P. (1999). Natural adjuvants: endogenous activators of dendritic cells. Nat. Med. *5*, 1249–1255.

Gao, Y., Nish, S.A., Jiang, R., Hou, L., Licona-Limón, P., Weinstein, J.S., Zhao, H., and Medzhitov, R. (2013). Control of T helper 2 responses by transcription factor IRF4-dependent dendritic cells. Immunity *39*, 722–732.

Gautier, E.L., Shay, T., Miller, J., Greter, M., Jakubzick, C., Ivanov, S., Helft, J., Chow, A., Elpek, K.G., Gordonov, S., et al.; Immunological Genome Consortium (2012). Gene-expression profiles and transcriptional regulatory pathways that underlie the identity and diversity of mouse tissue macrophages. Nat. Immunol. *13*, 1118–1128.

Ginhoux, F., Tacke, F., Angeli, V., Bogunovic, M., Loubeau, M., Dai, X.M., Stanley, E.R., Randolph, G.J., and Merad, M. (2006). Langerhans cells arise from monocytes in vivo. Nat. Immunol. *7*, 265–273.

Ginhoux, F., Liu, K., Helft, J., Bogunovic, M., Greter, M., Hashimoto, D., Price, J., Yin, N., Bromberg, J., Lira, S.A., et al. (2009). The origin and development of nonlymphoid tissue CD103+ DCs. J. Exp. Med. *206*, 3115–3130.

Ginhoux, F., Greter, M., Leboeuf, M., Nandi, S., See, P., Gokhan, S., Mehler, M.F., Conway, S.J., Ng, L.G., Stanley, E.R., et al. (2010). Fate mapping analysis reveals that adult microglia derive from primitive macrophages. Science *330*, 841–845.

Gosselin, D., Link, V.M., Romanoski, C.E., Fonseca, G.J., Eichenfield, D.Z., Spann, N.J., Stender, J.D., Chun, H.B., Garner, H., Geissmann, F., and Glass, C.K. (2014). Environment drives selection and function of enhancers controlling tissue-specific macrophage identities. Cell *159*, 1327–1340.

Guilliams, M., Ginhoux, F., Jakubzick, C., Naik, S.H., Onai, N., Schraml, B.U., Segura, E., Tussiwand, R., and Yona, S. (2014). Dendritic cells, monocytes and macrophages: a unified nomenclature based on ontogeny. Nat. Rev. Immunol. *14*, 571–578.

Heng, T.S., and Painter, M.W.; Immunological Genome Project Consortium (2008). The Immunological Genome Project: networks of gene expression in immune cells. Nat. Immunol. *9*, 1091–1094.

Hettinger, J., Richards, D.M., Hansson, J., Barra, M.M., Joschko, A.C., Krijgsveld, J., and Feuerer, M. (2013). Origin of monocytes and macrophages in a committed progenitor. Nat. Immunol. *14*, 821–830.

Hoeffel, G., Wang, Y., Greter, M., See, P., Teo, P., Malleret, B., Leboeuf, M., Low, D., Oller, G., Almeida, F., et al. (2012). Adult Langerhans cells derive predominantly from embryonic fetal liver monocytes with a minor contribution of yolk sac-derived macrophages. J. Exp. Med. *209*, 1167–1181.

Inaba, K., Inaba, M., Romani, N., Aya, H., Deguchi, M., Ikehara, S., Muramatsu, S., and Steinman, R.M. (1992). Generation of large numbers of dendritic cells from mouse bone marrow cultures supplemented with granulocyte/macrophage colony-stimulating factor. J. Exp. Med. *176*, 1693–1702.

Jiang, A., Bloom, O., Ono, S., Cui, W., Unternaehrer, J., Jiang, S., Whitney, J.A., Connolly, J., Banchereau, J., and Mellman, I. (2007). Disruption of E-cadherin-mediated adhesion induces a functionally distinct pathway of dendritic cell maturation. Immunity *27*, 610–624.

Lavin, Y., Winter, D., Blecher-Gonen, R., David, E., Keren-Shaul, H., Merad, M., Jung, S., and Amit, I. (2014). Tissue-resident macrophage enhancer landscapes are shaped by the local microenvironment. Cell *159*, 1312–1326.

Liu, K., Victora, G.D., Schwickert, T.A., Guermonprez, P., Meredith, M.M., Yao, K., Chu, F.F., Randolph, G.J., Rudensky, A.Y., and Nussenzweig, M. (2009). In vivo analysis of dendritic cell development and homeostasis. Science *324*, 392–397.

Lu, L., McCaslin, D., Starzl, T.E., and Thomson, A.W. (1995). Bone marrow-derived dendritic cell progenitors (NLDC 145+, MHC class II+, B7-1dim, B7-2-) induce alloantigen-specific hyporesponsiveness in murine T lymphocytes. Transplantation *60*, 1539–1545.

Lutz, M.B., Kukutsch, N., Ogilvie, A.L., Rössner, S., Koch, F., Romani, N., and Schuler, G. (1999). An advanced culture method for generating large quantities of highly pure dendritic cells from mouse bone marrow. J. Immunol. Methods *223*, 77–92.

Mayer, C.T., Ghorbani, P., Nandan, A., Dudek, M., Arnold-Schrauf, C., Hesse, C., Berod, L., Stüve, P., Puttur, F., Merad, M., and Sparwasser, T. (2014). Selective and efficient generation of functional Batf3-dependent CD103+ dendritic cells from mouse bone marrow. Blood *124*, 3081–3091.

McGovern, N., Schlitzer, A., Gunawan, M., Jardine, L., Shin, A., Poyner, E., Green, K., Dickinson, R., Wang, X.N., Low, D., et al. (2014). Human dermal $CD14^+$ cells are a transient population of monocyte-derived macrophages. Immunity *41*, 465–477.

McKenna, H.J., Stocking, K.L., Miller, R.E., Brasel, K., De Smedt, T., Maraskovsky, E., Maliszewski, C.R., Lynch, D.H., Smith, J., Pulendran, B., et al. (2000). Mice lacking flt3 ligand have deficient hematopoiesis affecting hematopoietic progenitor cells, dendritic cells, and natural killer cells. Blood *95*, 3489–3497.

Merad, M., Sathe, P., Helft, J., Miller, J., and Mortha, A. (2013). The dendritic cell lineage: ontogeny and function of dendritic cells and their subsets in the steady state and the inflamed setting. Annu. Rev. Immunol. *31*, 563–604.

Meredith, M.M., Liu, K., Darrasse-Jeze, G., Kamphorst, A.O., Schreiber, H.A., Guermonprez, P., Idoyaga, J., Cheong, C., Yao, K.H., Niec, R.E., and Nussenzweig, M.C. (2012). Expression of the zinc finger transcription factor zDC (Zbtb46, Btbd4) defines the classical dendritic cell lineage. J. Exp. Med. *209*, 1153–1165.

Mildner, A., Yona, S., and Jung, S. (2013). A close encounter of the third kind: monocyte-derived cells. Adv. Immunol. *120*, 69–103.

Miller, J.C., Brown, B.D., Shay, T., Gautier, E.L., Jojic, V., Cohain, A., Pandey, G., Leboeuf, M., Elpek, K.G., Helft, J., et al.; Immunological Genome Consortium (2012). Deciphering the transcriptional network of the dendritic cell lineage. Nat. Immunol. *13*, 888–899.

Naik, S.H., Metcalf, D., van Nieuwenhuijze, A., Wicks, I., Wu, L., O'Keeffe, M., and Shortman, K. (2006). Intrasplenic steady-state dendritic cell precursors that are distinct from monocytes. Nat. Immunol. *7*, 663–671.

Naik, S.H., Sathe, P., Park, H.Y., Metcalf, D., Proietto, A.I., Dakic, A., Carotta, S., O'Keeffe, M., Bahlo, M., Papenfuss, A., et al. (2007). Development of plasmacytoid and conventional dendritic cell subtypes from single precursor cells derived in vitro and in vivo. Nat. Immunol. *8*, 1217–1226.

Onai, N., Obata-Onai, A., Schmid, M.A., Ohteki, T., Jarrossay, D., and Manz, M.G. (2007). Identification of clonogenic common Flt3+M-CSFR+ plasmacytoid and conventional dendritic cell progenitors in mouse bone marrow. Nat. Immunol. *8*, 1207–1216.

Palucka, K.A., Taquet, N., Sanchez-Chapuis, F., and Gluckman, J.C. (1998). Dendritic cells as the terminal stage of monocyte differentiation. J. Immunol. *160*, 4587–4595.

Persson, E.K., Uronen-Hansson, H., Semmrich, M., Rivollier, A., Hägerbrand, K., Marsal, J., Gudjonsson, S., Håkansson, U., Reizis, B., Kotarsky, K., and Agace, W.W. (2013). IRF4 transcription-factor-dependent CD103(+)CD11b(+) dendritic cells drive mucosal T helper 17 cell differentiation. Immunity *38*, 958–969.

Pixley, F.J., and Stanley, E.R. (2004). CSF-1 regulation of the wandering macrophage: complexity in action. Trends Cell Biol. *14*, 628–638.

Sallusto, F., and Lanzavecchia, A. (1994). Efficient presentation of soluble antigen by cultured human dendritic cells is maintained by granulocyte/macrophage colony-stimulating factor plus interleukin 4 and downregulated by tumor necrosis factor alpha. J. Exp. Med. *179*, 1109–1118.

Sancho, D., Mourão-Sá, D., Joffre, O.P., Schulz, O., Rogers, N.C., Pennington, D.J., Carlyle, J.R., and Reis e Sousa, C. (2008). Tumor therapy in mice via antigen targeting to a novel, DC-restricted C-type lectin. J. Clin. Invest. *118*, 2098–2110.

Satpathy, A.T., Kc, W., Albring, J.C., Edelson, B.T., Kretzer, N.M., Bhattacharya, D., Murphy, T.L., and Murphy, K.M. (2012). Zbtb46 expression distinguishes classical dendritic cells and their committed progenitors from other immune lineages. J. Exp. Med. *209*, 1135–1152.

Schlitzer, A., McGovern, N., Teo, P., Zelante, T., Atarashi, K., Low, D., Ho, A.W., See, P., Shin, A., Wasan, P.S., et al. (2013). IRF4 transcription factor-dependent CD11b+ dendritic cells in human and mouse control mucosal IL-17 cytokine responses. Immunity *38*, 970–983.

Schraml, B.U., van Blijswijk, J., Zelenay, S., Whitney, P.G., Filby, A., Acton, S.E., Rogers, N.C., Moncaut, N., Carvajal, J.J., and Reis e Sousa, C. (2013). Genetic tracing via DNGR-1 expression history defines dendritic cells as a hematopoietic lineage. Cell *154*, 843–858.

Schulz, C., Gomez Perdiguero, E., Chorro, L., Szabo-Rogers, H., Cagnard, N., Kierdorf, K., Prinz, M., Wu, B., Jacobsen, S.E., Pollard, J.W., et al. (2012). A lineage of myeloid cells independent of Myb and hematopoietic stem cells. Science *336*, 86–90.

Serbina, N.V., Salazar-Mather, T.P., Biron, C.A., Kuziel, W.A., and Pamer, E.G. (2003). TNF/iNOS-producing dendritic cells mediate innate immune defense against bacterial infection. Immunity *19*, 59–70.

Shalek, A.K., Satija, R., Adiconis, X., Gertner, R.S., Gaublomme, J.T., Raychowdhury, R., Schwartz, S., Yosef, N., Malboeuf, C., Lu, D., et al. (2013). Single-cell transcriptomics reveals bimodality in expression and splicing in immune cells. Nature *498*, 236–240.

Shalek, A.K., Satija, R., Shuga, J., Trombetta, J.J., Gennert, D., Lu, D., Chen, P., Gertner, R.S., Gaublomme, J.T., Yosef, N., et al. (2014). Single-cell RNA-seq reveals dynamic paracrine control of cellular variation. Nature *510*, 363–369.

Son, Y.I., Egawa, S., Tatsumi, T., Redlinger, R.E., Jr., Kalinski, P., and Kanto, T. (2002). A novel bulk-culture method for generating mature dendritic cells from mouse bone marrow cells. J. Immunol. Methods *262*, 145–157.

Tamoutounour, S., Guilliams, M., Montanana Sanchis, F., Liu, H., Terhorst, D., Malosse, C., Pollet, E., Ardouin, L., Luche, H., Sanchez, C., et al. (2013). Origins and functional specialization of macrophages and of conventional and monocyte-derived dendritic cells in mouse skin. Immunity *39*, 925–938.

Vander Lugt, B., Khan, A.A., Hackney, J.A., Agrawal, S., Lesch, J., Zhou, M., Lee, W.P., Park, S., Xu, M., DeVoss, J., et al. (2014). Transcriptional programming of dendritic cells for enhanced MHC class II antigen presentation. Nat. Immunol. *15*, 161–167.

Xu, Y., Zhan, Y., Lew, A.M., Naik, S.H., and Kershaw, M.H. (2007). Differential development of murine dendritic cells by GM-CSF versus Flt3 ligand has implications for inflammation and trafficking. J. Immunol. *179*, 7577–7584.